



RESEARCH ARTICLE

# Green synthesis of silver nanoparticles using aqueous leaf extract of Bael (*Aegle marmelos* L.) and their antimicrobial and anticancer activities

Pillala Sai Kiran & Y Vimala\*

Department of Microbiology & Food Science and Technology, Gandhi Institute of Technology and Management (Deemed to be University),  
Visakhapatnam 530 045, India

\*Correspondence email - [vyapadin@gitam.edu](mailto:vyapadin@gitam.edu)

Received: 11 December 2023; Accepted: 11 June 2025; Available online: Version 1.0: 14 September 2025

**Cite this article:** Pillala SK, Vimala Y. Green synthesis of silver nanoparticles using aqueous leaf extract of Bael (*Aegle marmelos* L.) and their antimicrobial and anticancer activities. Plant Science Today (Early Access). <https://doi.org/10.14719/pst.3192>

## Abstract

This study presents a green synthesis approach for silver nanoparticles (AgNPs) using aqueous leaf extract of *Aegle marmelos*. This approach provides AgNPs with median size of 21 nm and plasmon resonance structures with a peak at 474 nm. The synthesized AgNPs were characterized using SEM EDX, FTIR, XRD and UV-Vis Spectrometer. The biosynthesis of AgNPs demonstrated notable antibacterial activity, with the highest zone of inhibition observed for *E. coli* ( $16.23 \pm 0.87$  mm) at a concentration of 150  $\mu\text{g/mL}$ . The AgNPs were further evaluated for their anticancer activity against HCT 116 cell lines and it was declared that the AgNPs were active against the cell lines with an IC<sub>50</sub> value of  $39.33 \pm 0.19$   $\mu\text{g/mL}$ . These findings suggest that AgNPs synthesised using *A. marmelos* extract possess promising antimicrobial and anticancer properties.

**Keywords:** Ag NPs; *Aegle marmelos*; anticancer activity; *E. coli*; green synthesis

## Introduction

In recent decades, pharmacological research has extensively explored the application of nanotechnology in healthcare. Materials with unusual physicochemical characteristics, such as enormous surface-to-volume ratios, ultra-small sizes, extremely reactive properties and distinctive interactions with structural elements like cores and emulsions that operate as carriers, as well as functional groups like medicinal compounds, are found within this scale. In the realm of medicine, nanotechnology focuses on materials with sizes between 1 and 100 nm for usage as drugs or as natural or synthetic polymer-loaded materials serving as carriers (1-2). Owing to their unique properties, nanomaterials have garnered significant attention from researchers worldwide (3). Nanomaterials are anticipated to find widespread applications in various sectors, including biological systems, electronics and optical communication (4). These programs are built on attributes such as their compact size, expansive surface area and physical attributes that provide room for numerous functions and customisation. Nanotechnology is a highly intriguing and rapidly developing topic in both medical and sustainable energy resources (5). Among metal NPs, AgNPs are particularly highly significant. These have a wide range of possible uses, including as air and water purifiers, antimicrobial agents and ink ingredients for inkjet printers. Among several of these intriguing qualities, the antibacterial property is well-known and crucial in various applications. Due to the

importance of Ag NPs, numerous research groups have explored various techniques for producing and stabilising nanoparticles for diverse applications. Wet synthesis techniques are generally classified into chemical and biological (green) methods. The natural substances found in plants and microbes have been widely employed in the more recent techniques to convert silver ions into metallic nanoparticles.

As an environmentally acceptable alternative to chemical synthesis, the manufacturing of nanoparticles has gained favour because it doesn't involve high energy consumption, excessive heat, or hazardous chemicals. Biomedical and food applications are also possible for nanoparticles produced using green methods. The creation of nanoparticles utilizing plant extracts has garnered attention recently due to its ease of use. Additionally, the procedures can be less expensive and are easily scalable. When creating nanoparticles, extracts from plants can be utilized as stabilizing and reducing agents. *Aegle marmelos*, a member of the family *Rutaceae*, is one among the traditional medicines used to treat deafness, diabetes, ophthalmia, asthma attacks and catarrh (6-7). *Aegle marmelos* as natural remedies are used to treat cardiovascular diseases, loose stools and stomach pain. Numerous prospective uses for Ag NPs have been rationally approved, including their effects on hypoglycemia, bitterness, antidiarrhea, antidysentery, demulcent, pain-relieving and gastroprotective qualities, as well as their use as antibiotics, injury-healing agents, repellents for insects and photocatalysts.

As a result, we report that by reducing a solution of silver nitrate using an aqueous extract of *Aegle marmelos* leaves, this work offers a straightforward and eco-friendly method for creating silver nanoparticles. The biological activities of silver nanoparticles, such as their antibacterial, antioxidant and cytotoxic capabilities, were also thoroughly examined.

## Materials and Methods

### Chemicals and reagents

Silver nitrate ( $\text{AgNO}_3$ , 99 % purity) was procured from HiMedia India Pvt Ltd. and used as received without further purification. *Aegle marmelos* leaves used in this experiment which were collected (in mid of June) in polyethylene bags from Tribal area around Araku valley in Visakhapatnam andhra Pradesh, India, washed thoroughly and cleaned again after being treated with  $\text{HgCl}_2$ .

### Preparation of leaf extract

*Aegle marmelos*'s fresh leaves (Fig. S1) were gathered and coarsely chopped. To get rid of any dust or additional particles that might have adhered to the leaf surface, these leaves were meticulously washed many times in double distilled water. Weigh 20 g of freshly cut *Aegle marmelos* leaves and then heat 200 mL of double-purified water to 60 °C for 60 min in an Erlenmeyer flask. This *Aegle marmelos* leaves extract was then filtered using Whatman No. 1 filter paper. The filtered material was used to create room-temperature nanoparticles and their capabilities were carefully investigated.

### Synthesis of silver nanoparticles

$\text{AgNO}_3$  was used as the raw material for the synthesis of AgNPs. In brief, a 0.1 M silver nitrate solution was prepared with distilled water. 25 mL of plant extract with 75 mL of  $\text{AgNO}_3$  solution was taken in a 250 mL beaker to support the formation of desirable AgNPs. The solution underwent a significant colour change within five minutes, transitioning from colourless to dark yellow, indicating the formation of AgNPs. After 10 min, the colour deepened further, turning dark brown. The UV-Vis spectra of the solution confirmed the reduction of silver ions. The synthesized NPs were separated from the mixture by centrifugation at 10,000 rpm for 20 minutes. This process was repeated three to four times to remove organic materials from the leaf extract. Pellet was carefully collected and dried at 60°C in a hot air oven for subsequent analysis. The product was subsequently dried at 60°C in a hot air oven and used for further analysis.

### Characterization of silver nanoparticles

The UV-Vis spectrum of the resulting AgNPs was analyzed to monitor the reduction of Ag ions. A Shimadzu 2600 UV-Vis spectrophotometer was used to record spectra within the 200–800 nm wavelength range. Functional groups responsible for the stabilization and reduction of AgNPs were identified through FTIR analysis with IR Prestige-21 Shimadzu in the range of 4000–500  $\text{cm}^{-1}$  with a resolution of 4  $\text{cm}^{-1}$ . The crystalline structure of the synthesised AgNPs was characterised using a D8-Bruker X-ray diffractometer with a  $2\theta$  scan of 10 to 90 degrees at a scan rate of 0.02 °/min. The morphology of the synthesized AgNPs was studied using scanning electron microscopy (SEM) at various magnifications, utilizing a JEOL JSM instrument with EDX for

elemental composition, operates at 0.5 to 30 kV with an ultimate resolution of 1.5 nm and a magnification range of 10x to 400000x.

### Antibacterial activity

The antibacterial effectiveness of the isolated compound was assessed using the agar well diffusion assay, which evaluates the compound's ability to inhibit bacterial growth based on the size of inhibition zones. Minimum inhibitory concentration (MIC) was not determined in this study, as agar diffusion does not provide the precision required for MIC quantification. Overnight cultures of *Pseudomonas aeruginosa* (MTCC-2295), *Escherichia coli* (MTCC-443), *Corynebacterium glutamicum* (MTCC-2745) and *Staphylococcus aureus* (MTCC-3160) were prepared in nutrient broth. Nutrient agar was prepared, autoclaved at 121°C and 15 psi for 15 minutes and poured aseptically into sterile petri plates. Antibacterial activity was tested using agar well diffusion, where DMSO served as the negative control and chloramphenicol (50  $\mu\text{L}$ ) as the positive control. Sterile glass spreaders were used to evenly inoculate the plates with bacterial cultures. Five wells of uniform diameter were punched using a sterile cork borer. Test compound solutions were prepared at concentrations of 80  $\mu\text{g}/\text{mL}$ , 100  $\mu\text{g}/\text{mL}$  and 150  $\mu\text{g}/\text{mL}$  and aliquots (usually 50  $\mu\text{L}$ ) were dispensed into each well. The plates were incubated at 37°C for 24 hours and zones of inhibition were measured in millimeters to assess antibacterial efficacy.

### Anticancer activity

A culture dish containing HCT 116 line cells was dissolved in Dulbecco's Improved Eagle's Medium (DMEM) using trypsin. Fifty millilitres of DMEM containing ten percent FCS (fetal calf serum) has been added to the broken-up cells in the flask. The cells were homogenized after being gently pipetted through the liquid to suspend them.

One millilitre of the crushed cell suspension was placed in every hole of a 24-well culture plate and various sample levels (10 to 200  $\mu\text{g}/\text{mL}$ ) were added. After that, the plate was kept in an incubator with humidified  $\text{CO}_2$  and 5%  $\text{CO}_2$  at 37°C. After being incubated for 48 hours, the cells were viewed under an x40 magnification inverted cultured tissue microscope (Olympus).

Tetrazolium bromide was used in the experiment (MTT assay). MTT is changed into a visible purple formazan by the succinate dehydrating agent and reductase found in live cells' mitochondria. The amount of cells that survive and the level of cytotoxicity are directly correlated with this formazan synthesis, while the latter is negatively correlated. Before adding MTT, each of the wells had been incubated for 48 hours. After that, they were let to rest at the room temperature for a period of three hours. Media was aspirated from each well. Every well's wavelength at 540 nm was measured using a Robonik optical analyzer following the formazan crystals' dissolution in 100 mL of DMSO. The formula (Eqn.1) below was used to get the percentage of development restriction (% IC):

$$(\% \text{ IC}) = \frac{\text{OD of Test}}{\text{OD of Control}} \times 100 \quad (\text{Eqn. 1})$$

The 50 % inhibition concentration ( $IC_{50}$ ) is often considered the most reliable biological indicator of cytotoxicity. The level of concentration of the pure substance that resulted in 50% of cell inhibition is represented by the  $IC_{50}$  value.

## Results and Discussion

### Extracellular synthesis of Ag NPs

This work examined in detail how Ag NPs are created extracellularly. After the plant extract was filtered, an  $AgNO_3$  solution was added to the filtrate and stirred for a few minutes. As seen in Fig. S2, the cell free filtrate's pale-yellow color changed to a dark brownish yellow colour, suggesting the creation of Ag NPs. Additionally, when temperature and incubation duration increased, the solution containing  $AgNO_3$  and plant extracts turned from a light brown colour into a dark brown color(8).

### Microscopic and elemental analysis

The size and form of Ag NPs isolated from an *A.marmelos* extract were assessed utilizing the scanning electron microscope (SEM). The silver nanoparticles, as reported by ImageJ, had a small proportion of longer particles and were spherical in shape, averaging 38 nm in diameter (Fig. 1). Green Ag NPs were generated with a diameter ranging from 60 to 120 nm, with a median diameter of 38 nm. The particles have spherical and cubic morphologies. The average size of green nanoparticles produced from silver nitrate and aloe vera was 70 nm(9). The green-synthesized Ag nanoparticles reported earlier (10) were spherical in shape, with diameters ranging from 20 to 150 nm.

### UV-Visible spectra of Ag NPs

UV-Vis absorption spectroscopy, which utilises the absorption spectrum, is a crucial biophysical method for monitoring the stability and production of green nanoparticles. Fig. 2 displays the absorption spectrum of Ag NPs, as determined by UV-Vis spectroscopy. This spectrum showed the greatest absorption

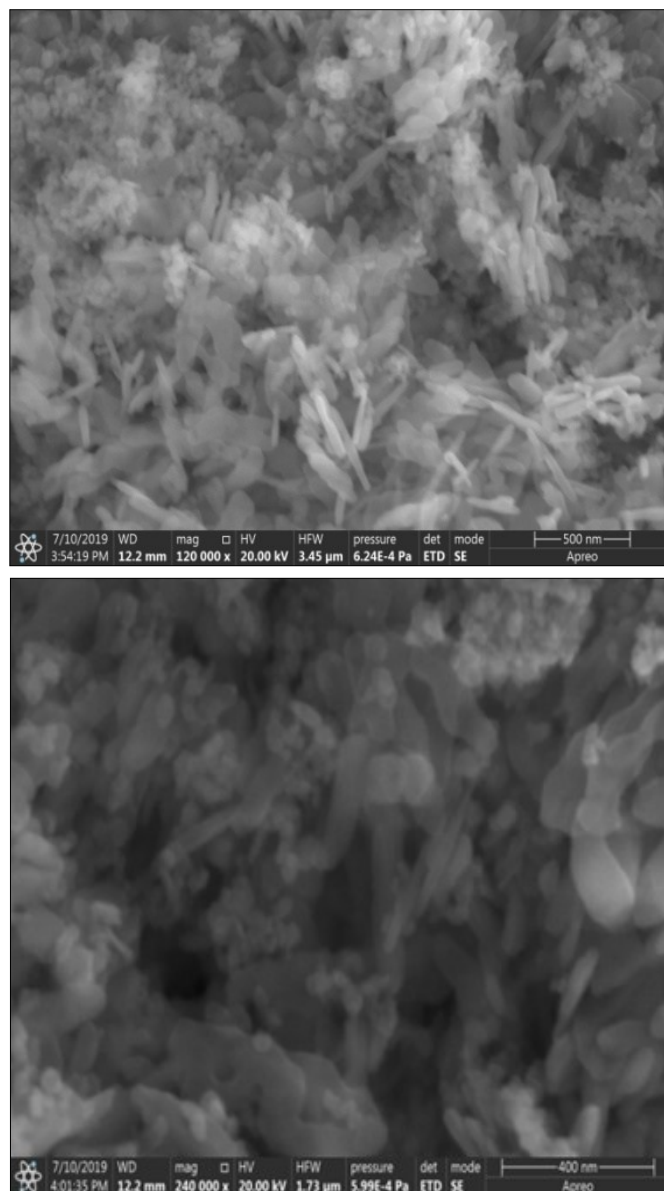


**Fig. 1.** SEM images of Ag NPs via *A.marmelos*

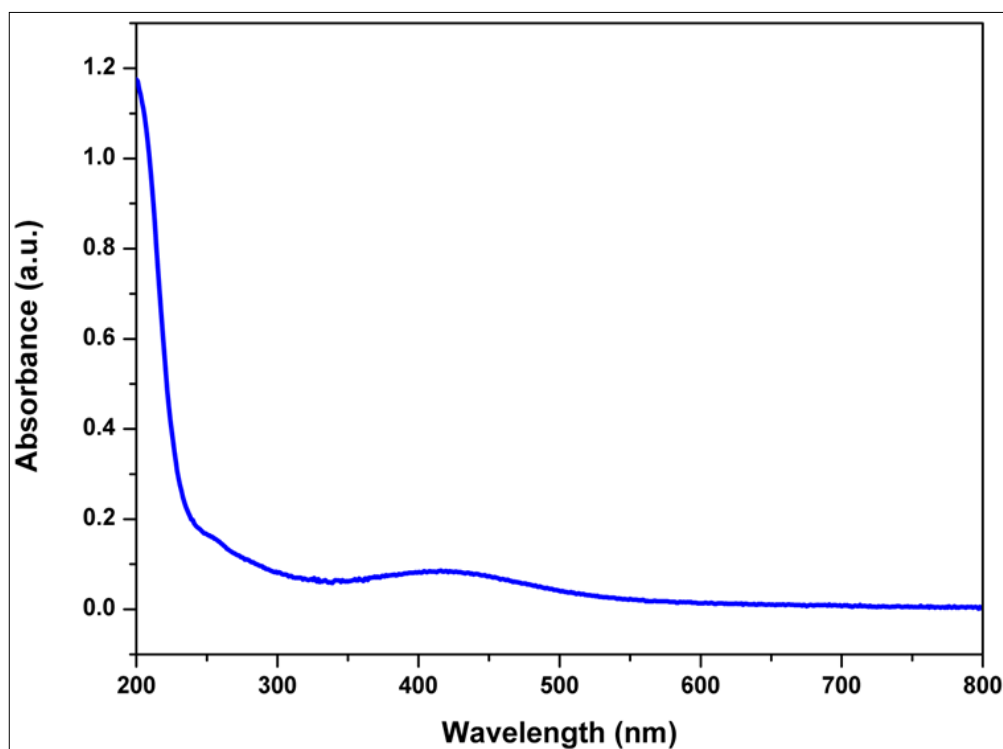


**Fig.2:** UV-Visible absorption spectra of AgNPs

peak, corresponding to the plasmon resonance, at 438 nm along with a broad peak. The Ag NPs solution exhibiting the highest absorbance spectrum at 200 nm was reported by using UV-Vis spectroscopy (9). A declining baseline correlates with smaller particle sizes, while a pronounced SPR peak at higher wavelengths suggests larger or aggregated particles (11). The process of creating Ag NPs is characterised by a bright and distinct colour.

#### FTIR analysis of Ag NPs

FTIR is an exact analytical technique that enables the identification and visualisation of individual components, their chemical structure, interactions with other substances, functional groups and bonding topologies. FTIR is used to analyse Ag NPs in order to identify the compounds that function as coating and stabilising agents and to measure the reduction of silver ions. The FTIR spectrum suggests that carboxylic acids and amide bonding could be the origin of the Ag NPs reduced or capped during green synthesis, as reported

earlier (12). Fig. 3a illustrates the FTIR spectra of the synthesized Ag NPs. The spectrum exhibits prominent absorption bands at approximately 3419, 1650 and 1489  $\text{cm}^{-1}$ . The band at 3419  $\text{cm}^{-1}$  corresponds to the O-H stretching vibrations associated with primary amines (12). The bands at 1650  $\text{cm}^{-1}$  and 1489  $\text{cm}^{-1}$  are indicative of the N-H stretching and bending vibrations, respectively (12).

#### X-ray diffraction analysis of Ag NPs

Fig. 3b displays the XRD peak characteristics of the Ag-NPs made using the green technique. Ag NPs have (111), (200), (220) and (311) facets in their face-centered cubic structure, respectively. These peaks may be seen at  $2\theta$  angles of  $38^\circ$ ,  $44.1^\circ$ ,  $64.4^\circ$  and  $77.4^\circ$  in the XRD spectrum. The crystalline character of the created Ag NPs is demonstrated by the fact that these diffraction peaks coincide with those of conventional Ag crystals. These outcomes demonstrate a close relationship with previous Ag NP-related research. Unassigned peaks in the XRD spectrum may be attributed to the

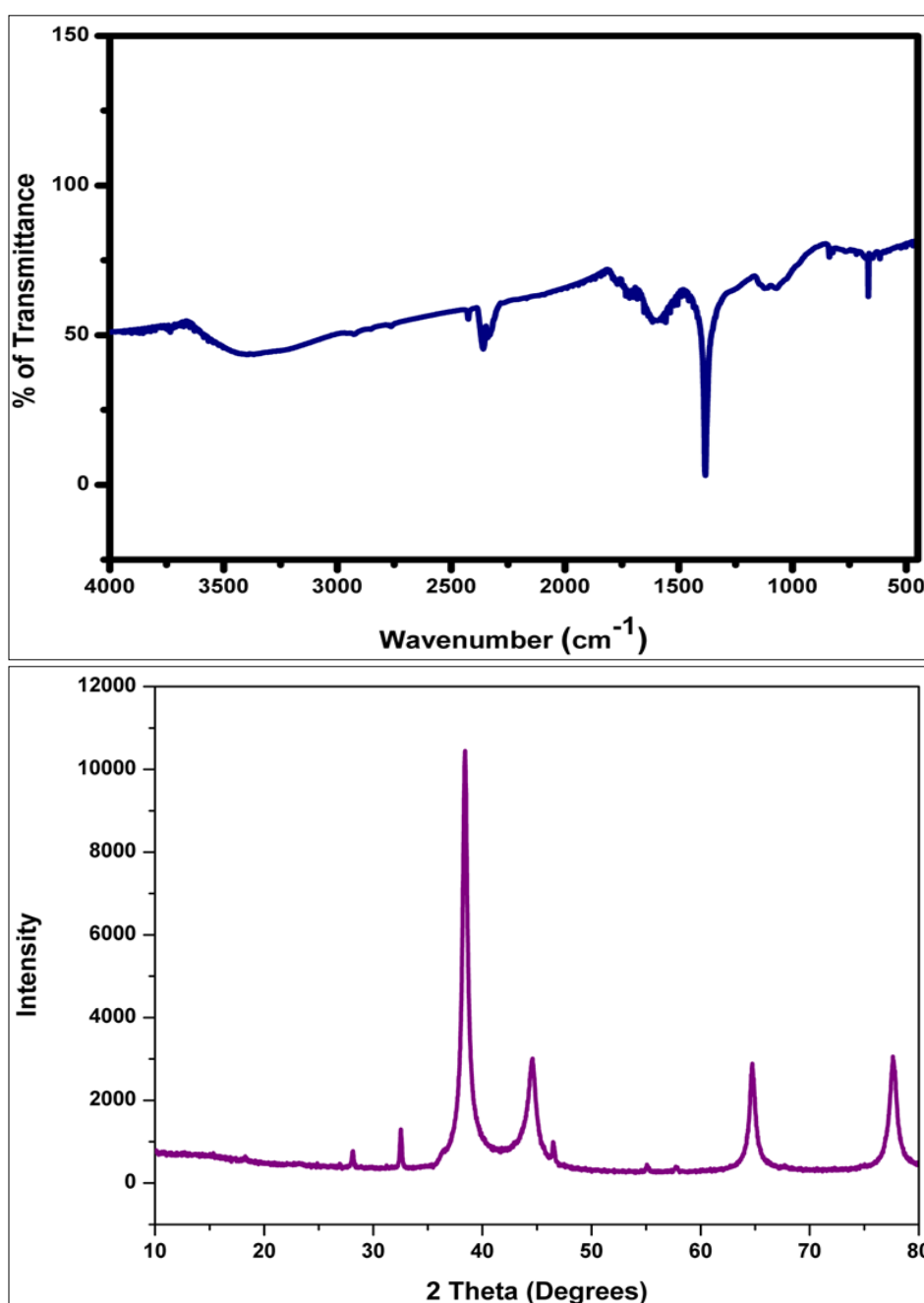


**Fig. 3a.** FTIR spectrum of prepared Ag NPs using *A. marmelos*; **b.** XRD arrangement of Ag NPs produced via extract from *Aegle marmelos* leaf



crystallization of plant-derived phytochemicals on the surface of Ag NPs during preparation of nanoparticles. The Debye-Scherrer formula (Eqn. 2) was used in this study to determine the average crystalline size (S) of the prepared Ag NPs, which was found to be 21.3 nm.

$$S = k\lambda/\beta\cos\theta \quad (\text{Eqn. 2})$$

Where, k is Scherrer's constant (0.9),  $\lambda$  denotes wavelength (1.54 Å), FWHM (full width at half maxima),  $\beta$  and  $\theta$  is diffraction angle.

### Antibacterial activity of AgNPs

Using the diffusion method on agar wells, AgNPs' antimicrobial effect towards the two species of bacteria was examined. Strong antibacterial action against all microbes (*P.aeruginosa*, *C. glutamicum*, *S.aureus* and *E.coli*) was shown by the green route produced AgNPs at all concentrations (80 (3), 100 (2) and 150 (1) µg/mL). It also demonstrated that processes affected the dose. AgNPs' antibacterial potential grew along with their concentration toward test microorganisms. At an amount of 150µg/mL, Ag NPs were shown to exhibit the maximum antimicrobial activity (16.23±0.87) towards *E.coli* (Fig. 4). These results were compared with previous reports (13).

### Anticancer activity of AgNPs

The biosynthesised Ag NPs were evaluated for anticancer activity against HCT 116 cell lines. The cytotoxicity was found to be concentration-dependent. The cytotoxicity of prepared Ag NPs on HCT 116 cell lines using MTT assay showed an IC<sub>50</sub> value of 39.33±0.19µg/mL (Table 2). The number of dead cells increased with the concentration of the purified compound. Analysis of the microscopic morphology in Fig. 5 revealed the morphological changes in cell lines treated with the purified compound. When observed under an inverted tissue culture microscope at 40x magnification, the treated cells exhibited shrinkage and detachment from the substratum, indicating apoptosis or cell death.

## Conclusion

This study reports, for the first time, the synthesis of Ag NPs using aqueous leaf extract of *A. marmelos* and AgNO<sub>3</sub>. These Ag NPs are small, inexpensive and easy to synthesise, exhibiting therapeutic efficacy against various cancer cell lines and microbial pathogens. These green pathways, which generated Ag NPs, were first visually recognised by looking for a change in colour. Then, several characterization techniques were used to demonstrate the presence of Ag NPs. XRD investigations and absorption spectra confirmed the existence of Ag NPs. The spherical shape and size of the un-agglomerated Ag NPs, which are roughly 38 nm in average size, were validated by electron microscope techniques, such as SEM examination. The findings showed that diffused green Ag NPs produced by *Aegle marmelos* extract had stronger anticancer activity on the HCT 116 cancer cell line than chemically produced AgNPs. The AgNPs exhibited dose-dependent cytotoxicity, with an IC<sub>50</sub> value of 39.33 µg/mL against HCT116 cells. With less cytotoxicity toward healthy cells, the extract from *Aegle marmelos* incorporating AgNPs may potentially be an alternate treatment option for human cancer. We recognize the importance of comparing the antibacterial activity of the plant extract with the synthesized AgNPs to determine whether nanoparticle synthesis enhances antimicrobial efficacy. A comparative analysis was conducted to highlight the enhanced antibacterial efficacy following nanoparticle synthesis. The zone of inhibition results indicate that AgNPs exhibit a dose-dependent antibacterial effect against all tested pathogens. While AgNPs show notable activity, the positive control (30 µg/mL standard antibiotic) demonstrated the highest inhibition. The comparison with *Aegle marmelos* extract has been added to highlight the augmentation of antibacterial activity through nanoparticle synthesis.

**Table 1.** Antibacterial activity of Ag NPs against bacteria

S.No	Test organism	Zone of inhibition (mm)			
		AgNPs (µg/mL)			Positive control 30µg/mL
		80	100	150	
1	<i>P. aeruginosa</i>	8.16±0.76	10.76±1.25	14.23±0.83	18.83±2.02
2	<i>C. glutamicum</i>	9.43±1.42	12.23±0.83	15.86±0.41	19.86±1.89
3	<i>S.aureus</i>	10.43±0.72	12.33±0.67	13.46±0.22	17.66±1.68
4	<i>E.coli</i>	12.14±0.56	14.37±1.23	16.23±0.87	21.83±2.05

**Table 2.** In-vitro cytotoxicity of AgNPs on HCT 116 Cell lines (Mean of three replicates ± Standard deviation)

S.No	Ag NPs (mg/mL)	% Cell viability (HCT 116 cell lines)	
1	0		100.00
2	12.5		61.5±0.5
3	25		52.52±0.75
4	50		42.80±0.51
5	75		39.32±0.05
6	100		36.08±0.02
7	150		31.80±0.51
8	200		21.52±0.03
9	IC <sub>50</sub>		39.33±0.19

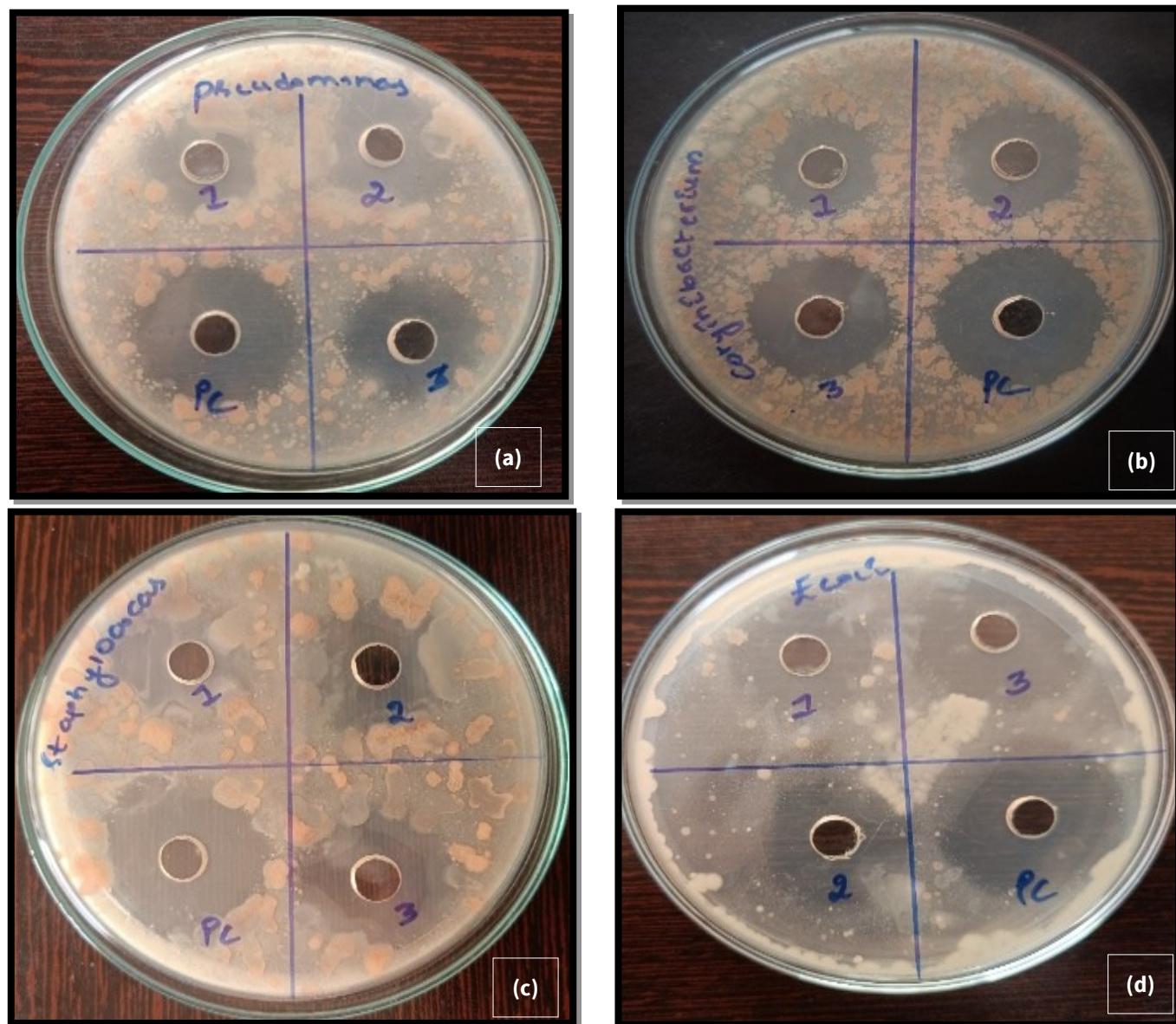


**Fig. 4.** Antibacterial activity of Ag NPs against (a) *P.aeruginosa*(b) *C.glutamicum*(c) *S.pyogenes* and (d) *E.coli*

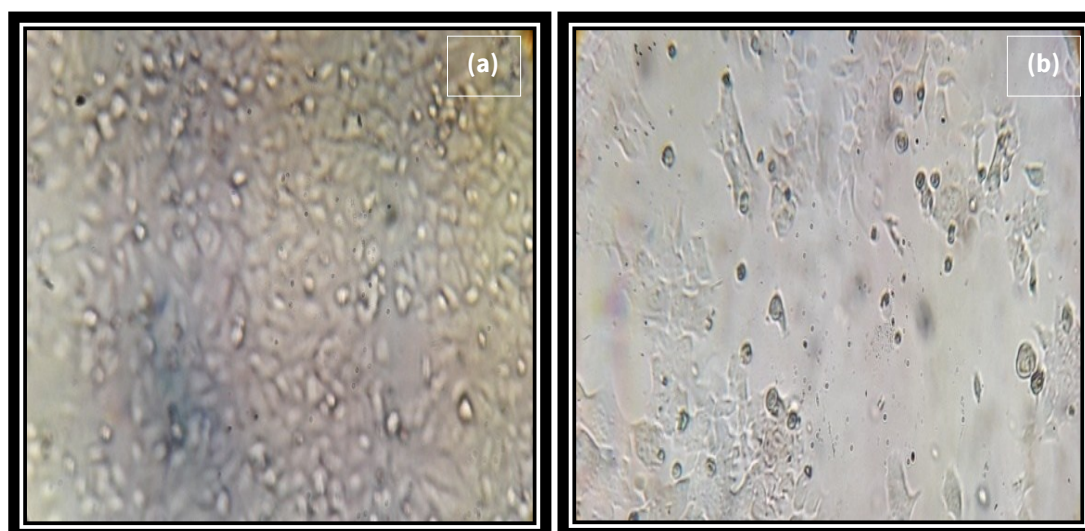


**Fig. 5.** (a) Control and (b) Treatment with Ag NPs

### Acknowledgements

Not Applicable

### Authors' contributions

PS developed the methodology and prepared the original manuscript draft. YV conceptualized the study and provided overall supervision. All authors read and approved the final version of the manuscript. .

## Compliance with ethical standards

**Conflict of interest:** The Authors do not have any conflicts of interest to declare.

**Ethical issues:** None

## References

1. Vidya Sagar PSR, Ramadevi D, Basavaiah K, Botsa SM. Green synthesis of silver nanoparticles using aqueous leaf extract of *Saussurea obvallata* for efficient catalytic reduction of nitrophenol, antioxidant and antibacterial activity. *Water Sci Eng*. 2024;17(3):274–82. <https://doi.org/10.1016/j.wse.2023.09.004>
2. Zhang L, Gu FX, Chan JM, Wang AZ, Langer RS, Farokhzad OC. Nanoparticles in medicine: therapeutic applications and developments. *Clin Pharmacol Ther*. 2008;83:761–9. <https://doi.org/10.1038/sj.clpt.6100400>
3. Senol AM, Metin O, Acar M, Onganer Y, Meral K. The interaction of fluorescent Pyronin Y molecules with monodisperse silver nanoparticles in chloroform. *J Mol Struct*. 2016;1103:212–6. <https://doi.org/10.1016/j.molstruc.2015.09.037>
4. Darder M, Colilla M, Ruiz-Hitzky E. Chitosan-clay nanocomposites: applications as electrochemical sensors. *Appl Clay Sci*. 2005;28:199–208. <https://doi.org/10.1016/j.clay.2004.02.009>
5. Chou CS, Chen CY, Lin SH, Lu WH, Wu P. Preparation of TiO<sub>2</sub>/bamboo-charcoal-powder composite particles and their applications in dye-sensitized solar cells. *Adv Powder Technol*. 2015;26:711–7. <https://doi.org/10.1016/j.appt.2014.12.013>
6. Rao PK, Babu BV, Krishna AR, Reddi MS, Mohan BS, Devi KA, Susmitha U, Rao R. Green synthesis of silver nanoparticles using *Litsea glutinosa* leaves and stem extracts and their antibacterial efficacy. *J Water Environ Nanotechnol*. 2022;7(4):363–9. <https://doi.org/10.22090/jwent.2022.04.003>
7. Rao KJ, Paria S. Green synthesis of silver nanoparticles from aqueous *Aegle marmelos* leaf extract. *Mater Res Bull*. 2013;48(2):628–34. <https://doi.org/10.1016/j.materresbull.2012.11.035>
8. Mohan KK, Sinha M, Mandal BK, Ghosh AR, Siva KK, Sreedhara PR. Green synthesis of silver nanoparticles using *Terminalia chebula* extract at room temperature and their antimicrobial studies. *Spectrochim Acta A Mol Biomol Spectrosc*. 2012;91:228–33. <https://doi.org/10.1016/j.saa.2012.02.001>
9. Kumar TVC, Prasad TNVKV, Adilaxmamma K, Alpharaj M, Muralidhar Y, Prasad PE. Novel synthesis of nanosilver particles using plant active principle aloin and evaluation of their cytotoxic effect against *Staphylococcus aureus*. *Asian Pac J Trop Dis*. 2014;4(1):92–6. [https://doi.org/10.1016/S2222-1808\(14\)60421-7](https://doi.org/10.1016/S2222-1808(14)60421-7)
10. Firdhouse MJ, Lalitha P, Sripathi SK. Novel synthesis of silver nanoparticles using leaf ethanol extract of *Pisonia grandis* (R. Br). *Der Pharma Chemica*. 2012;4(6):2320–6.
11. Khan M, Khan M, Adil SF, Tahir MN, Tremel W, Alkhathlan HZ. Green synthesis of silver nanoparticles mediated by *Pulicaria glutinosa* extract. *Int J Nanomedicine*. 2013;8:1507–16. <https://doi.org/10.2147/IJN.S43309>
12. Silva LP, Pereira TM, Bonatto CC. Frontiers and perspectives in the green synthesis of silver nanoparticles. In: Shukla AK, Irvani S, editors. *Green synthesis, characterization and applications of nanoparticles*. 2019. p.137-64. <https://doi.org/10.1016/B978-0-08-102579-6.00007-1>
13. Guzman M, Dille J, Godet S. Synthesis and antibacterial activity of silver nanoparticles against gram-positive and gram-negative bacteria. *Nanomedicine*. 2012;8:37–45. <https://doi.org/10.1016/j.nano.2011.05.007>

## Additional information

**Peer review:** Publisher thanks Sectional Editor and the other anonymous reviewers for their contribution to the peer review of this work.

**Reprints & permissions information** is available at [https://horizonpublishing.com/journals/index.php/PST/open\\_access\\_policy](https://horizonpublishing.com/journals/index.php/PST/open_access_policy)

**Publisher's Note:** Horizon e-Publishing Group remains neutral with regard to jurisdictional claims in published maps and institutional affiliations.

**Indexing:** Plant Science Today, published by Horizon e-Publishing Group, is covered by Scopus, Web of Science, BIOSIS Previews, Clarivate Analytics, NAAS, UGC Care, etc See [https://horizonpublishing.com/journals/index.php/PST/indexing\\_abstracting](https://horizonpublishing.com/journals/index.php/PST/indexing_abstracting)

**Copyright:** © The Author(s). This is an open-access article distributed under the terms of the Creative Commons Attribution License, which permits unrestricted use, distribution and reproduction in any medium, provided the original author and source are credited (<https://creativecommons.org/licenses/by/4.0/>)

**Publisher information:** Plant Science Today is published by HORIZON e-Publishing Group with support from Empirion Publishers Private Limited, Thiruvananthapuram, India.